Journal of the Korean Nuclear Society
Volume 31, Number 2, pp.139~150, April 1999

Swelling Pressures of a Potential Buffer Material for High-Level Waste Repository

Jae Owan Lee, Won Jin Cho, and Kwan Sik Chun
Korea Atomic Energy Research Institute
150 Dukjin-dong, Yusong-gu, Taejon 305-353, Korea

jolee@nanum.kaeri.re.kr

(Received April 9, 1998)

Abstract

The swelling pressure of a potential buffer material was measured and the effect of dry density, bentonite content and initial water content on the swelling pressure was investigated to provide the information for the selection of buffer material in a high-level waste repository. Swelling tests were carried out according to Box-Behnken' s experimental design. Measured swelling pressures were in the wide range of 0.7 Kg/cm^2 to 190.2 Kg/cm^2 under given experimental conditions. Based upon the experimental data, a 3-factor polynomial swelling model was suggested to analyze the effect of dry density, bentonite content and initial water content on the swelling pressure. The swelling pressure increased with an increase in the dry density and bentonite content, while it decreased with increasing the initial water content and, beyond about 12 wt.% of the initial water content, levelled off to nearly constant value.

Key Words : swelling pressure, bentonite, buffer material, repository

1. Introduction

One of the major functions of buffer in a high-level waste repository is to play a role of self-sealing. The buffer closes any voids and cracks in the repository thereby to restrict the intrusion of ground water and to retard the release of radionuclides from radioactive waste to the surrounding environment.

Bentonite-based materials are widely favored as the buffer material, because they have high swelling potential, high sorptive capacity, and good durability under disposal environment. In Sweden[1], Finland[2], and Japan[3] have considered Na-bentonite, in France[4], Swiss[5] and Spain[6] Ca-bentonite, and in Canada[7] a mixture of 50% Na-bentonite and 50% sand, for the use of buffer materials in their natural repositories.

The swelling capacity of buffer material should be high for its successful sealing role as a barrier, and on the other hand, its swelling pressure be low to avoid excessive load to container and the surrounding rock. When a bentonite-based

material is used for the buffer, it therefore is essential to investigate its swelling pressure.

The swelling pressure is one which the bentonite acts on a system with limited space upon its contact with water. Many investigators[8-13] reported that the swelling pressure was in the wide range of 0.27 Kg/cm^2 to 590.45 Kg/cm^2 depending upon dry density, bentonite content, initial water content, ionic strength, and temperature.

This study is intended to investigate the swelling characteristics of a domestic bentonite-based material which could be considered as a candidate buffer material for a high-level waste repository in Korea. The swelling pressure is measured, and based upon the measured experimental data, a 3-factor polynomial model is proposed and the effect of dry density, bentonite content and initial water content on the swelling pressure is analyzed.

2. Mechanism of Swelling

Swelling requires a force of repulsion separating bentonite particles to increase the volume upon their contact with water. The process can be visualized as the result of repulsions between adjacent bentonite particles or their interamellar layers : elastic rebound from unbending of the particles, hydration of the particle surface and of the exchangeable cations, and osmotic swelling due to electrical double layer repulsion. In a confining system with no release of a load, the initial small rebound may be ignored and the hydration and the electrical double layer repulsion dominate the swelling process.

When the bentonite is in contact with water, the water, in the first stage, is adsorbed in successive monolayers on the surface and exchangeable cations and pushes apart the particles or the layers of a montmorillonite which is a major constituent of the bentonite. The second stage of swelling is osmotic process in which the particles or the layers may be pushed further apart due to double layer repulsion. This osmotic swelling occurs since the water tends to equalize the high concentration of ions between two particles or layers, which are so close together that their double layers overlap, and the low concentration of ions in bulk pore water.

The total amount of swelling, i.e., the swelling pressure is determined by combination of hydration force and osmotic force. However, it is not easy to predict the swelling pressure precisely because it depends upon whether each force can be calculated. Although the force of hydration, as indicated by Thomson and Ali[14], is considered to be dominant in the swelling at low water contents, it cannot be quantitively predicted so far. When the plate distance exceeds about 10 angstroms (equivalent with four adsorbed layers of water), diffusive ion layers form adjacent to the plate and the osmotic pressure becomes the major repulsive force in swelling. The concentration of ions is higher in the plane midway between particles or layers than they are in the bulk pore water. Water moves in response to the concentration gradient and exerts a force tending to move the particles further apart. The osmotic force operates over longer distance and is a very important source of swelling, particuly at higher water contents[15]. Its magnitude may be predicted assuming simple models.

3. Experimental

3.1. Materials

Bentonite : The bentonite used was taken from Jinmyeong mine which is located in Yangnam Kyungsangbuk-do. It was air-dried and passed through No. 200 of ASTM(American Society for Testing and Materials) standard sieves. The X-ray

Table 1. Chemical Composition of the Bentonite.

Chemical constituent	SiO_2	Al_2O_3	Fe_2O_3	CaO	MgO	K_2O	Na_2O
Percentage (%)	57.36	21.27	6.43	2.36	2.25	0.98	2.98

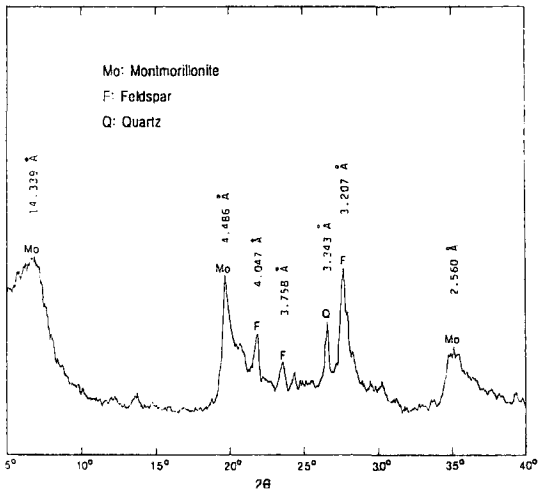

Fig. 1. X-ray Diffraction Pattern of the Bentonite

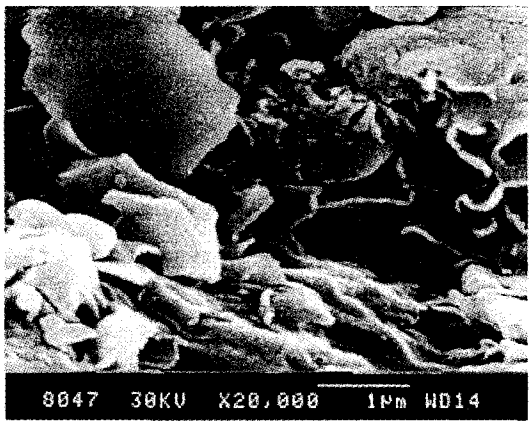

(a) SEM micrograph

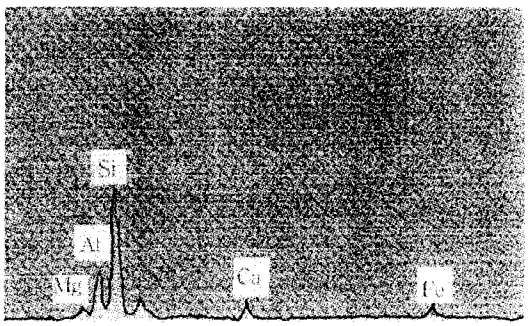

(b) EDX pattern

Fig. 2. Results of SEM and EDX Analysis for the Bentonite

diffraction pattern is shown in Fig. 1 and the results of SEM(Scanning Electron Microscope) and EXD(Energy Dispersive X-ray) analysis in Fig. 2. The bentonite was found to be of Ca-type and its mineralogical composition was 64.7% montmorillonite, 34.3% feldspar, and 1.00% quartz. The chemical composition is shown in Table 1. The surface area and the cation exchange capacity were 361 m^2/g and 47.7 meq/100g, respectively. The free swell index measured by Forster's method was 89.1 ± 2.8 mL/10g.

Bentonite-Sand Mixture : This is prepared by adding the sand of No. 6 which is produced for industrial use by Daekwang mining company, to the above mentioned bentonite. The sand included quartz as a major mineral and a small amount of feldspar and mica. The chemical composition of the sand was shown in Table 2, and its particle size distribution was shown in Table 3. The specific gravity of the sand was 2.65 Mg/m^3.

Water : Distilled and deionized water was used for the swelling tests.

Table 2. Chemical Composition of the Sand.

Chemical constituent	SiO_2	Al_2O_3	Fe_2O_3	CaO	MgO	K_2O	Na_2O
Percentage (%)	82.32	9.78	1.32	0.48	0.31	3.55	1.46

Table 3. Particle Size Distribution of the Sand

Sieve no.	#16	#30	#40	#50	#100	#140	#200
Wt. percentage (%)	100	99.92	97.39	59.71	6.36	1.14	0.21

3.2. Experimental Procedures

Preparation of compacted samples

The bentonite sample was oven-dried at 105 ℃ and weighed in a given mass. The water was added to the weighed sample using ultrasonic sprayer to adjust a desired water content. After the adjustment of water content, the sample was put into a polyethylene zip-bag and kept in a desiccator for overnight to give uniform distribution of the sprayed water in the sample. Then, the known mass of sample was compacted uniaxially into a stainless steel cylindrical mold to a given dry density, and again was left in a desiccator for 24 hours to reach equilibrium.

Measurement of swelling pressures

The swelling pressures were measured using an experimental apparatus shown in Figure 3. The apparatus includes four sections : main test section, pressurized water-feeding section, vacuuming section, and signal and data processing section. The main test section consists of a stainless steel cylindrical cell of which the dimension was 5×10^{-2} m in height and 5×10^{-2} m in diameter, porous metal filters to avoid the loss of bentonite particles, and swelling pressure sensors mounted in both vertical and horizontal

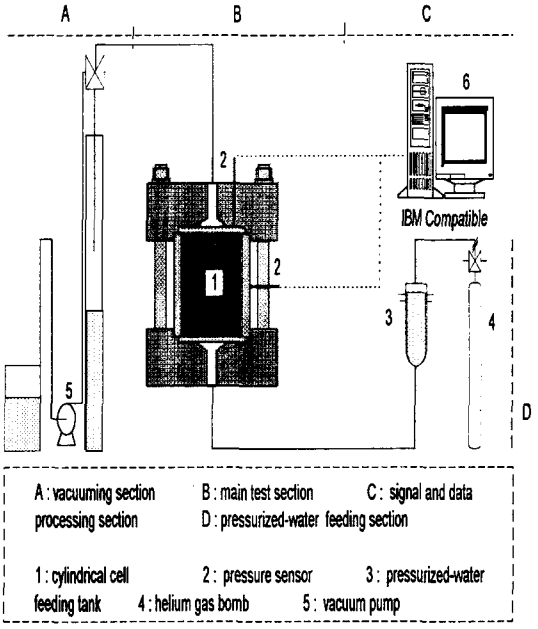

Fig. 3. Experimental Apparatus for Measuring the Swelling Pressures

directions. The pressurized water-feeding section consists of a stainless steel reservoir and a highly pressurized helium gas bomb which is used for feeding the water in the reservoir to the compacted sample. The stainless steel reservoir is designed to tolerate the pressure of 30 Kg/cm^2. In

the vacuuming section, a vacuum pump was connected to the outlet of the main test section to pull out the air entrapped in the compacted sample. The signal and data processing section is designed to acquire swelling pressures from pressure sensor and then to display their values on digital indicator.

The swelling pressures were measured according to experimental design which had three levels to each of the following three variables : dry density, bentonite content, and initial water content. Although a total of 27 test runs(=3×3×3) were needed to investigate the effect of the variables on the swelling pressure, for the optimization of the test runs, the present study employed Box-Behnken' s experimental design [16] in which 15 of 27 test runs were conducted. Table 4 shows experimental conditions designed according to the Box-Behnken' s scheme for the measurement of the swelling pressures.

These swelling tests start with feeding the pressurized water after the zero point of pressure sensor was adjusted, and the swelling pressures sent from the sensor were collected in a given time interval using personal computer. The swelling pressures are effective ones which are obtained by subtracting an applied pressure from the collected swelling pressures. These tests are performed at 20℃, and proceed until the swelling pressure reaches steady-state.

Fabric Analysis of Compacted Bentonite by Means of SEM

The fabric of compacted bentonite was analyzed with scanning electron microscope (SEM). The cylindrical samples of the compacted bentonite, prepared as for the swelling pressure tests, were oven-dried and axially split across a diameter using the principles of the Brazilian split tension test [17]. This produced tensile fracture faces at 90° to the axis of compaction. The samples were trimmed to fit on the SEM specimen stud and attached using a rapid adhesive. The surfaces to be analyzed were stripped using transparent, adhesive tape, and the specimen was rendered electrically conductive by gold coating.

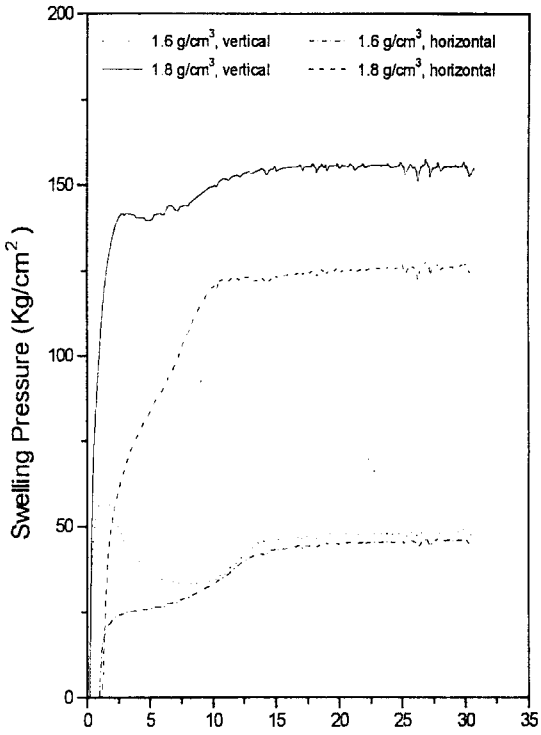

Fig. 4. Development of Swelling Pressure Versus Elapsed Time for 100% Bentonite

4. Results and Discussion

4.1. Experimental Swelling Pressures

Fig. 4 is an example to represent the change of swelling pressures with the contacting time of sample and water. As shown in the figure, the swelling pressures develop rapidly until they reach

Table 4. Box-Behnken' s Experimental Design and Measured Swelling Pressures

ID	Experimental conditions			Measured swelling pressures	
	Box-Behnken Design no.	Dry density (Mg/m^3)	Bentonite content (%)	Water content (%)	Vertical (Kg/cm^2)	Horizontal (Kg/cm^2)
1	13	1.6	65	10	5.84	5.53
2	10	1.6	100	6	50.11	33.76
3	3	1.4	100	10	6.62	9.54
4	9	1.6	100	14	36.68	34.68
5	1	1.8	100	10	143.52	114.59
6	12	1.6	30	6	1.16	1.53
7	8	1.4	65	6	2.81	4.16
8	6	1.8	65	6	21.23	20.24
9	4	1.4	30	10	0.96	0.56
10	11	1.6	30	14	1.10	0.98
11	7	1.4	65	14	1.39	2.12
12	15	1.6	65	10	5.84	5.53
13	2	1.8	30	10	1.36	2.88
14	5	1.8	65	14	27.16	23.06
15	14	1.6	65	10	5.84	5.53

a peak in a few days. Subsequently, the swelling pressures start to decline gradually to a constant value. These tests ended in 30 days because the time-dependent behavior of the swelling pressure was regarded as reaching steady-state. The swelling pressures obtained are listed in Table 4, together with experimental conditions. Both vertical and horizontal swelling pressures showed similar trends in the time-dependent behavior. The vertical swelling pressures were higher than the horizontal ones, suggesting the anisotropic nature of the compacted sample.

4.2. Parametric Modelling of the Swelling Pressure

When the dry density, the bentonite content, and the initial water content are considered as experimental variables affecting the swelling pressure, the relationship between the swelling pressure and three experimental variables may be expressed in a polynomial. The following quadratic equation is used to approximate most of experimental data properly [18].

$$\begin{aligned} P_s &= f(x_1, x_2, x_3) \\ &= b_o + \sum_{i=0}^{3} b_i x_i + \sum_{i=0}^{3} b_{ii} x_{ii}^2 + \sum_{\substack{i=0 \\ i<j}}^{3} b_{ij} x_i x_j \\ &= b_o + b_1 x_1 + b_2 x_2 + b_3 x_3 + b_{11} x_1^2 + b_{22} x_2^2 \\ &\quad + b_{33} x_3^2 + b_{12} x_1 x_2 + b_{13} x_1 x_3 + b_{23} x_2 x_3 \end{aligned} \quad (1)$$

where P_s is the swelling pressure, $x1$ the dry density, $x2$ the bentonite content, $x3$ the initial water content, and b the coefficient of the quadratic equation.

The coefficients of the quadratic equation were determined through multiple regression analysis of experimental data, in which the experimental swelling pressures were employed as log P_s to

minimize the deviation in the calculation. The multiple regression analysis was conducted using LOTUS 123 program. The coefficients of the quadratic equation calculated are given :

$b_0 = 0.766$ $b_1 = 0.457$
$b_2 = 0.753$ $b_3 = -0.045$
$b_{11} = 0.001$ $b_{22} = 0.006$
$b_{33} = 0.070$ $b_{12} = 0.296$
$b_{13} = 0.103$ $b_{23} = -0.028$

Correlation coefficient, $R^2 = 0.99$

That is, the swelling pressure is expressed in the following polynomial as a function of dry density, bentonite content, and initial water content.

$$\log P_s = 0.766 + 0.457 x_1 + 0.753 x_2 - 0.045 x_3 + 0.001 x_1^2 + 0.006 x_2^2 + 0.070 x_3^2 + 0.296 x_1 x_2 + 0.103 x_1 x_3 - 0.028 x_2 x_3 \quad (2)$$

This equation explains that the dry density and bentonite content give positive and large contribution to the swelling pressure, whileas the initial water content gives negative and small one. In Table 5, the experimental P_s values and calculated ones from the above equation (2) are compared, which shows a relatively good agreement.

4.3. Discussion

The effect of dry density, bentonite content, and initial water content on the swelling pressure was carried out using the proposed polynomial equation (2).

Effect of dry density

Fig. 5. is the swelling pressure as a function of dry density. The swelling pressure was in the range of 0.7 Kg/cm^2 to 190.2 Kg/cm^2 and increased with increasing the dry density. The dependence of the swelling pressure upon the dry density was more sensitive in higher dry density.

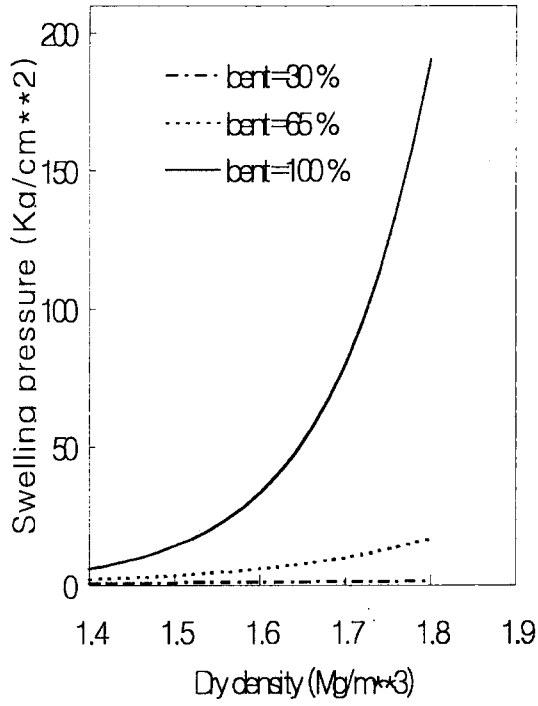

Fig. 5. Effect of Dry Density on the Swelling Pressure

Using the concept of effective bentonite dry density [19], an attempt was made to explain the relationship between swelling pressure and dry density. The effective bentonite dry density, ρ_{eff} is defined as the ratio of the mass of bentonite to the volume of bentonite plus void in the mixture :

$$\rho_{eff} = \frac{mass\ of\ bentonite}{volume\ of\ bentonite\ plus\ void\ in\ the\ mixture} = \frac{(1-\omega_s)\,\rho_{md}}{1-\omega_s(\rho_{md}/\rho_s)} \quad (3)$$

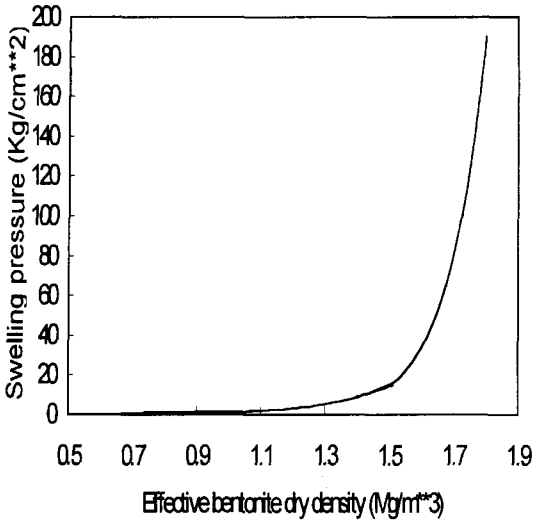

Fig. 6. Swelling Pressure as a Function of Effective Clay Dry Density

where ω_s is the weight fraction of sand in the mixture, ρ_{md} the dry density of the mixture, and ρ_s the true density of sand.

The effective bentonite dry densities which correspond to the dry densities in the Fig. 5 are calculated using the equation (3). The swelling pressure versus the effective bentonite dry densities are plotted in Fig. 6. As shown in the figure, the relationship between swelling pressure and dry density can be explained by the concept of effective clay dry density. This suggests that the swelling pressure for the mixture of bentonite and sand is dominated by the bentonite. The sand acts merely as an inert filler material and serves only to limit the free volume into which the bentonite can be compacted. Therefore, when the effective bentonite dry density of mixture is similar to the dry density of pure bentonite, then the swelling pressure is close to that for the pure bentonite.

(a) dry density = 1.6Mg/m^3

(b) dry density = 1.8Mg/m^3

Fig. 7. Results of SEM Analysis of the Compacted Bentonite with the Dry Densities of 1.6Mg/m^3 and 1.8Mg/m^3

Fig. 6 also shows that there is a slow increase of the swelling pressure up to a threshold dry density between 1.6 Mg/m^3 and 1.8 Mg/m^3. Above the threshold dry density, the swelling pressure rises at a much steeper gradient. Such a behavior of the swelling pressure was also reported in Gray et al.'s experiment with Avonseal bentonite-sand mixture[20], in which

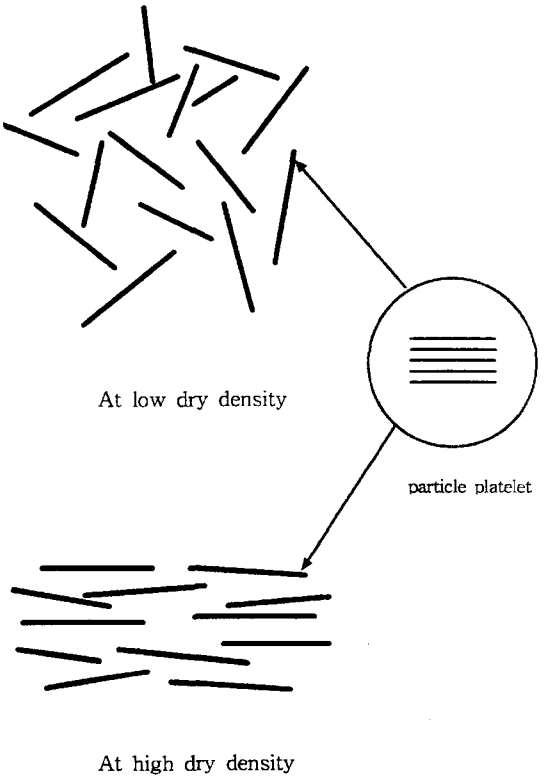

Fig. 8. Schematic Representation of the Fabric of Compacted Bentonite with the Change of Dry Density

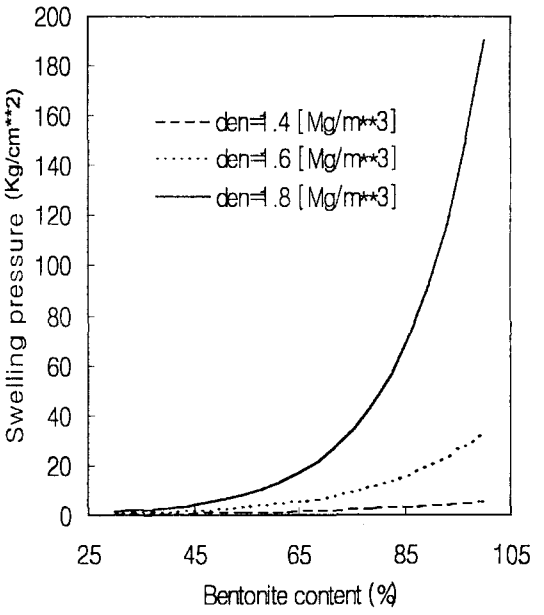

Fig. 9. Effect of Bentonite Content on the Swelling Pressure

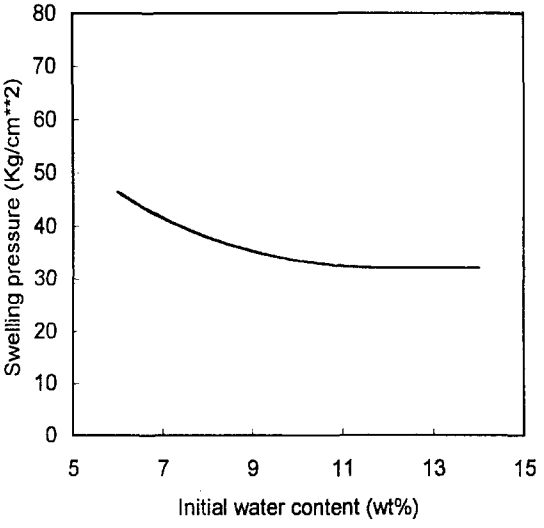

Fig. 10. Effect of Initial Water Content on the Swelling Pressure for the 100% Bentonite(ρ_d=1.6Mg/m^3)

the threshold dry density was found to be between 1.6 Mg/m^3 and 1.7 Mg/m^3. The steep increase of the swelling pressure beyond the threshold dry density is supposed to be due to the anisotropic nature of the compacted bentonite. The SEM analysis may offer an explanation for the anisotropy. The typical micrographs of the compacted bentonite, when compacted to 1.6 Mg/m^3 and to 1.8 Mg/m^3, are presented in Fig. 7(a) and 7(b), respectively. Fig. 7(a) shows that the mixture at low effective dry density consists of randomly arranged aggregates of bentonite particles (micropeds), while Fig. 7(b)

shows that, at the dry densities above the threshold value, interparticle voids are mostly eliminated, the micropeds become fused, and the topography is relatively uniform. In Fig. 8 is given a schematic representation of the fabric of compacted bentonite with the change in the dry density. The results of SEM analysis suggest that the micropeds of bentonite particles beyond the threshold dry density are arranged in a nearly parallel orientation and thus the corresponding swelling pressures increase steeply. On the other hand, Pusch put out for this phenomenon in his report[21] the explanation that the force of hydration on the surface of particles or their interlamellar layers may be of significance in the swelling pressure of highly compacted bentonite with the densities of 2.0 - 2.1 Mg/m^3.

Effect of bentonite content

The effect of bentonite content on the swelling pressure is plotted in Fig. 9. As shown in the figure, the swelling pressure increases with increasing the bentonite content, which is at a slow gradient up to about 50 wt% of bentonite content. Above 50 wt%, there is a rapid increase in the swelling pressure. Such a behavior gets distinct at higher dry density. It is suggested for the mixture of bentonite and sand that the swelling pressure is controlled largely by the bentonite content.

Effect of initial water content

Fig. 10 represents the effect of initial water content on the swelling pressure of bentonite with the dry density of 1.6 Mg/m^3. The swelling pressure, which is in the range of from 32.1 Kg/cm^2 to 46.5 Kg/cm^2, decreases with increasing initial water content. From about 12wt% of initial water content, however, there is little change in the swelling pressure. This is expected to be because the bentonite contacting with the initial water is partially swelled prior to swelling pressure test. Therefore, the lower the initial water content is, the higher the swelling pressure is.

5. Conclusions

The swelling pressure was in the range of 0.7 Kg/cm^2 to 190.2 Kg/cm^2 under given experimental conditions. The vertical swelling pressure was higher than the horizontal one, the difference of which increased with increasing the dry density.

A 3-factors polynomial model was suggested as follows :

$$\log P_s = 0.766+0.457\,x_1+0.753\,x_2-0.045\,x_3+0.001\,x_1^2 +0.006\,x_2^2+0.070\,x_3^2+0.296\,x_1\,x_2+0.103\,x_1\,x_3 -0.028\,x_2\,x_3$$

The swelling pressure increased with an increase in the dry density, and the relationship of swelling pressure versus dry density for various bentonite contents, for the mixture, could be explained by the concept of effective clay dry density. The swelling pressure also increased with increasing the bentonite content. On the contrary, it decreased with initial water content and, beyond about 12wt% of initial water content, levelled off to nearly constant value.

The experimental results obtained will be useful to the selection of a candidate buffer material for a high-level waste repository in Korea.

References

1. SKBF/KBS, "Final Storage of Spent Fuel - KBS-3" (1983).
2. T. Vieno, A. Hautojarvi, L. Koskinen, and H. Nordman, "TVO-92 Safety Analysis of Spent

Fuel Disposal," Report VTJ-92-33E, Technical Research Center of Finland (1992).
3. PNC, "Research and Development on Geological Disposal of High-Level Radioactive Waste," PNC TN1410 93-059 (1992).
4. H. Coulon, A. Lajudie, P. Debrabant , R. Atabek, M. Jordia, and R. Andre Jehan, "Choice of French Clays as Engineered Barrier Components for Waste Disposal," In Scientific Basis for Nuclear Waste Management X, pp. 813-824 (1987).
5. NAGRA, "Project Gewahr 1985, Nuclear Waste Management in Switzland : Feasibility Studies and Safety Analysis," Project Report NAGRA-NTB-85-09(1985).
6. J. Linares et al., "Spanish Research Activities in the Field of Backfilling and Sealing: A Preliminary Study of Some Spanish Sedimentary (Madrid Basin) and Hydrothermal (Almeria) Bentonite," Proc. of an NEA/CEC Workshop on Sealing of Radioactive Waste Repositories," pp. 318-332, Paris (1989).
7. L. H. Johnson, J. C. Tait, D. W. Shoeesmith, J. L. Crosthwaite and M. N. Gray, "The Disposal of Canada' s Nuclear Fuel Waste: Engineering Barrier Alternative," Atomic Energy of Canada Limited Report, AECL-10718, COG-93-8 (1994).
8. W. J. Cho, K. S. Chum, J. O. Lee, and M. J. Kang, "Analysis of Functional Criteria for Buffer Material in the High-Level Waste Repository," KAERI/TR-933/97, Korea Atomic Energy Research Institute (1997).
9. J. H. Westsik, L. A. Bray, F. N. Hodges, and E. J. Wheelwright, "Permeability, Swelling and Radionuclide Retardation Properties of Candidate Backfill Materials," the Sci. Basis for Nuclear Waste Management (1982).
10. L. Borgesson and R. Pusch, "Rheological Properties of a Calcium Smectite," SKB Tech. Rep. 87-31 (1987).
11. M. N. Gray, S. C. H. Cheung, and D. A. Dixon, "The Influence of Sand Content on Swelling Pressures and Structure Developed in Statically Compacted Na-Bentonite," AECL-7825 (1984).
12. D. A. Dixon and M. N. Gray, " The Engineering Properties of Buffer Material - Research at Whiteshell Nuclear Research Establishment," AECL TR-350, pp. 513-529 (1985).
13. R. N. Yong, P. Boonsinsuk and G. Wong, "Development of Backfill Material for a Nuclear Fuel Waste Vault," AECL TR-350, pp. 561-594 (1985).
14. S. Thomson and P. Ali, "A Laboratory Study of the Swelling Properties of Sodium and Calcium Modifications of Lake Edmonton Clay," Proc. 2nd Int. Res. and Eng. Conf. Expansive Soils, Texas A&M University, pp. 256-262 (1969).
15. R. M. Hardy, "Identification and Performance of Swelling Soils Types," Canadian Geotech. J., Vol. 11, No. 2 (1965).
16. G. E. P. Box and D. W. Behnken, "Some New Three Level Designs for the Study of Quantitative Variables," Technometrices, Vol. 2, No. 4, pp. 455-475 (1960).
17. A. M. Neville, "Properties of Concrete," Pitman Publishing, London (1980).
18. D. C. Montgomery, "Design and Analysis of Experiments," John Wiley & Sons, pp. 445-497 (1984).
19. D. A. Dixon, M. N. Gray and A. W. Thomas, "A Study of the Compaction Properties of Potential Clay-Sand Buffer Mixtures for Use in Nuclear Fuel Waste Disposal, "Engineering Geology, 21, pp. 247-255 (1985).
20. M. N. Gray, S. C. H. Cheung and D. A.

Dixon, "Swelling Pressures of Compacted Bentonite/Sand Mixtures," AECL TR-350, pp. 776-785, Canada (1985).
21. R. Pusch, "Water Uptake Migration, and Swelling Characteristics of Unsaturated and Saturated Highly Compacted Bentonite," SKBF/KBS Teknisk Rapport 80-11 (1980).